Predicting the piezoresistance contribution of carbon nanotubes in a polymer matrix through finite element modeling

A.I. Oliva-Avilés and V. Sosa
Centro de Investigación y de Estudios Avanzados, Unidad Mérida, Departamento de Física Aplicada, Apartado Postal 73-Cordemex, 97310, Mérida, Yucatán, México.
e-mail: andresivan19@hotmail.com

F. Avilés
Centro de Investigación Científica de Yucatán, Unidad de Materiales, Calle 43, No. 130 Col. Chuburná de Hidalgo, 97200, Mérida, Yucatán, México.

Received 2 May 2012; accepted 25 June 2013

The change in electrical resistance due to mechanical deformation of carbon nanotube (CNT)/polymer composites can be rationalized in terms of two main effects: i) changes in the composite electrical resistivity due to changes in the CNT network configuration, and ii) deformation of the CNTs themselves. The contribution of CNT dimensional changes (ii) to the piezoresistivity of CNT/polymer composites is investigated here. A model based on a representative volume element which describes the CNT geometrical contribution to the composite electromechanical response (piezoresistivity) in terms of the CNT and matrix deformations is proposed. Finite element analysis is performed to correlate the macroscale composite strain to the individual CNT strain. The CNT geometric contribution to the piezoresistivity of the composite is quantified for a range of matrix elastic modulus and different CNT orientations. Based on the model predictions and previous experimental results, it is estimated that the contribution of the CNT deformation to the composite piezoresistivity is only about 5%, indicating that the dominant effect in the piezoresistivity of CNT/polymer composites is the change in the CNT network configuration.

Keywords: Carbon nanotubes; piezoresistivity; polymer composites; finite element.

PACS: 73.63.Fg; 72.80.Tm; 72.20.Fr.

1. Introduction

About a decade ago, a reversible correlation between the mechanical strain and the electrical resistance of individual singlewall carbon nanotubes (SWCNTs) was discovered [1,2], implying their use as strain sensors. Dharap *et al*. used the strain sensing capabilities of SWCNTs to develop a SWCNT film (buckypaper) for strain sensing [3]. They reported a nearly linear relationship between the measured voltage change and the applied strain, in the film elastic range ($< 0.04\%$ of strain), for their SWCNT films, implying the potential use of such films as multidirectional and multiple location strain sensors. Due to their outstanding physical properties (*i.e.* mechanical, electrical and thermal properties), CNTs can be exploited for the design of polymer composite materials with novel multifunctionality in terms of conductivity and strain sensing capabilities [4-6]. Zhang *et al.* reported that multiwall(MW) CNT/polymer composites at 5% weight content can be utilized as strain sensors with piezoresistive sensitivity ~ 3.5 times higher than that of a traditional metallic strain gage [4]. Kang *et al.* reported the piezoresistive behavior of SWCNT/polymethyl methacrylate composite films at 10% weight percentage in constructing a "neuron sensor" [5]. The authors also developed a "biomimetic artificial neuron" by extending the length of such a sensor to a long continuous strain sensor. In the last years, CNT alignment inside liquid solutions and polymers has emerged as a highly desirable feature for the fabrication of CNT materials and nanostructured devices with tailored properties. Mechanical [6-11], magnetic [12-14] and electrical techniques [15-20] have been recently investigated for manipulating CNTs in polymers and other viscous media.

It has been shown that MWCNT alignment increases the range of the linear response of the piezoresistive signal in the alignment direction and also increases the piezoresistive sensitivity of the material compared to the case where the CNTs are randomly oriented [21]. The piezoresistive behavior observed in all of these CNT/polymer composites may be attributed mainly to two mechanisms that occur while strain is applied [22,23]: (i) a variation in the configuration of the CNT conductive network, and (ii) the dimensional changes of the CNTs themselves due to the CNT deformation. The former effect is considered to be caused by variations in the interparticle distance, CNT-to-CNT contact resistance and tunneling effects between neighbor CNTs [22-25], while the latter is a merely geometric effect of the CNT. According to modeling studies [22-25], it is generally accepted that the variation on the configuration of the CNT conductive network is the main responsible for the piezoresistivity of CNT/polymer composites, but the geometric contribution of the CNT deformation is still subject of investigation. Dharap *et al*. [3] reported that for a SWCNT film (buckypaper), the change in electrical resistance due to variations in the CNT film dimensions are in a lower proportion ($\sim 12\%$) than the changes in the intrinsic resistivity ($\sim 88\%$) indicating the changes in the intrinsic film resistivity to be dominant. Wichmann *et al*., however, suggested that the geometric contribution to the piezoresistivity of their MWCNT/epoxy compos-

ites is on the same order as the contribution related to the tunneling resistance [26]. It is thus clear that the quantification of the contribution of the CNT deformation to the piezoresistivity of CNT/polymer composites is still an unresolved issue. To this aim, a simple finite element model based on a representative volume element (RVE) of the CNT/polymer composite is developed here to calculate the strain experienced by the CNT when the composite is deformed. This CNT strain is then used to estimate the change in electrical resistance yielded by the composite due solely to the CNT dimensional changes. The dependence of such a CNT geometric contribution for composites with different CNT weight fractions, matrix elastic modulus and degree of CNT orientation is investigated.

2. Piezoresistive and strain analyses

2.1. Piezoresistive model

In a conductive material the electrical resistance R can be expressed in terms of its geometry and its intrinsic electrical resistivity ρ by means of the equation [27],

$$R = \rho \frac{L}{A} \tag{1}$$

where L and $A = wt$ are the length and cross sectional area of the material respectively, with w being its width and t its thickness. When the material is subjected to strain, changes in its electrical resistance are therefore related to changes in its geometry (L and A) and/or changes in its intrinsic electrical resistivity ρ.

From Eq. (1) and assuming that the resistivity of the undeformed/initial (ρ_i) and deformed/final (ρ_f) configurations is the same (ρ_i= ρ_f= ρ), the relative change of electrical resistance ($\Delta R/R_i = (R_f - R_i)/R_i$) of a percolated CNT/polymer composite due to an applied unidirectional axial deformation can be expressed as,

$$\frac{\Delta R}{R_i} = \frac{L_f w_i t_i}{L_i w_f t_f} - 1 \tag{2}$$

Using the definition of infinitesimal strain ($\varepsilon_x = (L_f - L_i)/L_i$) and Poisson's ratio ($\nu$ = -$\varepsilon_y/\varepsilon_x$, where the axes are defined in Fig. 1) and considering that the material is isotropic, the final length (L_f), width (w_f) and thickness (t_f) after deformation (see Fig. 1) can be expressed as a function of their initial (sub-index "i") values as,

$$L_f = L_i\,(1 + \varepsilon_x) \tag{3}$$

$$w_f = w_i\,(1 - \nu\varepsilon_x) \tag{4}$$

$$t_f = t_i\,(1 - \nu\varepsilon_x) \tag{5}$$

Substituting Eqs. (3-5) into Eq. (2) yields,

$$\frac{\Delta R}{R_i} = \frac{1 + \varepsilon_x}{(1 - \nu\varepsilon_x)^2} - 1 \tag{6}$$

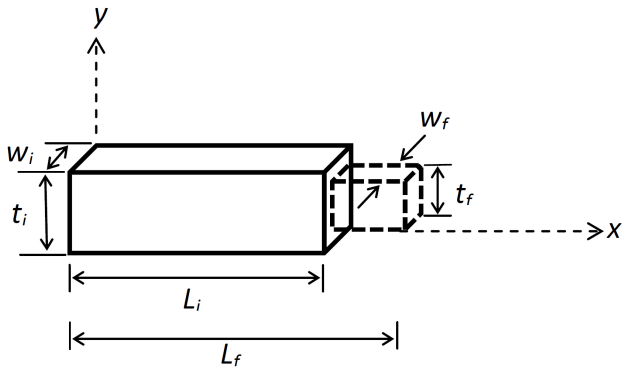

FIGURE 1. Schematic of the material unidirectional axial deformation.

Eq. (6) relates the relative change of the electrical resistance to the dimensional changes (axial strain) of the material. Since this equation was derived assuming that ρ is constant, it isolates the geometric contribution of the strained material to its piezoresistivity, $i.e.$ it corresponds to the effect of merely changing the dimensions of the strained material. For the case of a CNT/polymer composite, this is equivalent to neglect all piezoresistive contributions from the variation in the configuration of the CNT network and assuming that all changes are due to the geometric effect caused by the deformation of CNT, transferred by the matrix. However, due to the insulating nature of the considered polymer matrices, the electrical resistance changes of the composite material can be attributed solely to the conductive CNTs. Therefore, the strain ε_x in Eq. (6) corresponds to the axial strain of the CNT (ε_{CNT}) embedded in the polymer. Substituting ε_x by ε_{CNT} in Eq. (6) and recasting in terms of a new parameter α = $\varepsilon_{\text{CNT}}/\varepsilon_{\text{APPL}}$ yields,

$$\frac{\Delta R}{R_i} = \frac{1 + \alpha\varepsilon_{\text{APPL}}}{(1 - \nu\alpha\varepsilon_{\text{APPL}})^2} - 1 \tag{7}$$

where $\varepsilon_{\text{APPL}}$ is the macroscale axial strain applied to the whole composite material. The amount of strain that the CNT actually experiences (ε_{CNT}) when the composite material is axially strained by $\varepsilon_{\text{APPL}}$ is only a fraction of the $\varepsilon_{\text{APPL}}$, and the introduction of the parameters α and $\varepsilon_{\text{APPL}}$ allows this quantification. α is therefore ≤ 1 and it depends on the relation between the lengths of the CNT and matrix. The limiting (ideal) case α = 1 occurs when both the CNT and matrix have the same length (continuous CNT). To compute α, a finite element analysis (FEA) was conducted as detailed in the next section.

2.2. Prediction of carbon nanotube deformation by finite element analysis

2.2.1. Representative volume element

Square RVEs were constructed for CNT/polymer composites with 0.5 and 2 CNT weight percentage (wt%), Fig. 2.

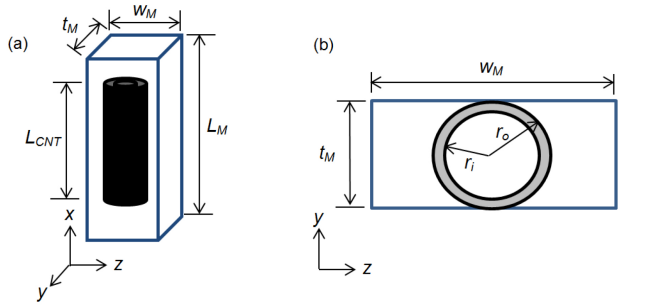

FIGURE 2. RVE for the analysis of CNT/polymer composites. (a) 3D view, (b) top view.

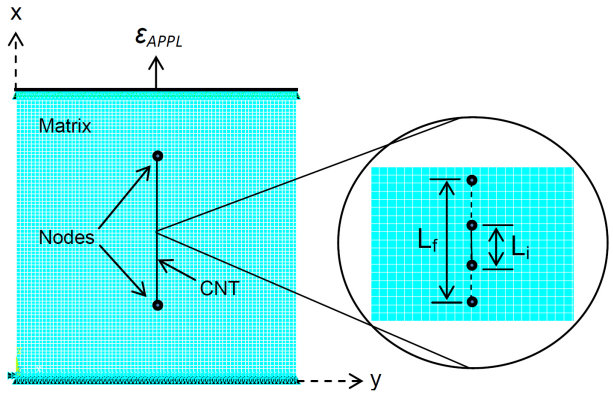

FIGURE 3. Finite element model of a CNT/polymer composite under axial strain..

ing to Chen *et al.*, square RVEs are preferred over cylindrical to obtain more accurate results [28]. As observed in Fig. 2(a), a CNT of length L_{CNT} is embedded in a non-conductive matrix of length L_M, where $L_M \geq L_{\text{CNT}}$. The CNT and matrix were assumed to be perfectly bonded. CNT dimensions used were fixed to r_o= 6.5 nm, r_i= 2 nm, see Fig. 2(b), and L_{CNT} = 1 μm. L_M and w_M were varied while t_M was kept equal to the external diameter of the CNT, $2r_o$, Fig. 2(b). L_M was systematically varied in relation to L_{CNT} (= 1 μm) from L_{CNT}/L_M= 0.1 to L_{CNT}/L_M= 1. In order to keep a constant CNT weight fraction, w_M needs to be varied along with L_{CNT}/L_M according to,

$$w_M = \frac{\pi\left(r_o^2 - r_i^2\right)}{8r_o}\left(\frac{1-V}{V}\right)\left(\frac{L_{\text{CNT}}}{L_M}\right) \qquad (8)$$

where V is the composite volume fraction. The matrix and CNT densities used were 0.8065 g/cm^3 and 1.4 g/cm^3, respectively [29,30].

2.2.2. *Finite element analysis*

FEA was used to compute the strain experienced by the CNT embedded in the matrix when the composite is subjected to $\varepsilon_{\text{APPL}}$, and hence α in Eq. (7). A commercial software (ANSYS 12.0) was employed for the analysis and a representative finite element model as presented in Fig. 3. The matrix was modeled using two-dimensional structural solid elements ("PLANE 42") with four-node elements (one at each node corner) and two degrees of freedom (DOF) at each node (translation in the nodal x and y directions). For modeling the CNT, a one-dimensional structural element ("LINK 1") was used, which is a uniaxial tension-compression element with two DOFs at each node, which are compatible with those of PLANE 42. The matrix and CNT were modeled as perfectly bonded, which means that the two nodes located at the ends of the CNT coincide with nodes belonging to the polymer matrix. Based on an initial convergence analysis, the matrix was constructed using models of around 1 million elements. The CNT elastic modulus was assumed to be E_{CNT}=1 TPa, which is a typically accepted value in the literature [28,30,31]. Both the CNT and matrix were considered to have a Poisson ratio of ν = 0.3. LINK 1 requires the definition of a spring constant K, which is expressed in terms of the CNT geometry and elastic modulus as $K = A_{\text{CNT}}E_{\text{CNT}}/L_{\text{CNT}}$, where A_{CNT}= $(\pi/4)(r_o^2 - r_i^2)$. The selected values for the parametric study of the matrix elastic modulus were 0.1, 1 and 10 GPa, in order to investigate the influence of the matrix stiffness on the piezoresistive effect. The influence of the CNT degree of alignment respect to the direction of applied strain (x) was also investigated by rotating the CNT one-dimensional element.

To compute α, the composite was subjected to a fixed unidirectional strain in the x direction ($\varepsilon_{\text{APPL}}$, see Fig. 3). Nodes at the bottom edge (x= 0), were constrained to have zero displacement in the x and y directions while nodes at the top edge were coupled in the y DOF in order to promote a state of uniform strain. The CNT elongation was computed by the difference of the displacements of the nodes located at the CNT ends ($L_f - L_i$, see inset in Fig. 3). Thus, the CNT strain (ε_{CNT}) was calculated dividing the CNT elongation by the CNT initial length (ε_{CNT}= $(L_f - L_i)/L_i$).

3. Results and discussion

3.1. Influence of L_{CNT}/L_M

Finite element analysis was conducted to study the influence of the L_{CNT}/L_M ratio on the CNT deformation. The elastic modulus of the matrix was E_M= 1 GPa and the applied strain $\varepsilon_{\text{APPL}}$= 2%. Figure 4 shows the relative CNT strain (α, see Eq. (7)) as a function of L_{CNT}/L_M for composites with 0.5 and 2 wt%.

Regardless of the CNT weight loading, for L_{CNT}/L_M ratios up to 0.9 the CNT strain is lower than 11% of the whole composite strain ($\alpha \leq 0.11$). For L_{CNT}/L_M =1 (a composite with "continuous reinforcement"), it is observed that α suddenly reaches 1, which means that both CNT and composite are subjected to the same strain for such a case. These results can be explained in terms of the large difference in stiffness between the CNT and matrix, and the discrete length of the CNT. Unless the CNT continuously span along the length of the matrix, the strain applied to the composite causes only a small CNT deformation since the CNT elastic modulus is

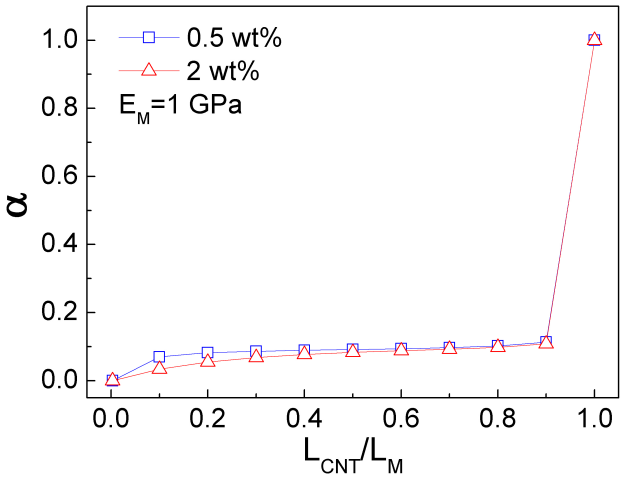

FIGURE 4. α vs L_{CNT}/L_M for CNT composites with 0.5 and 2 wt%.

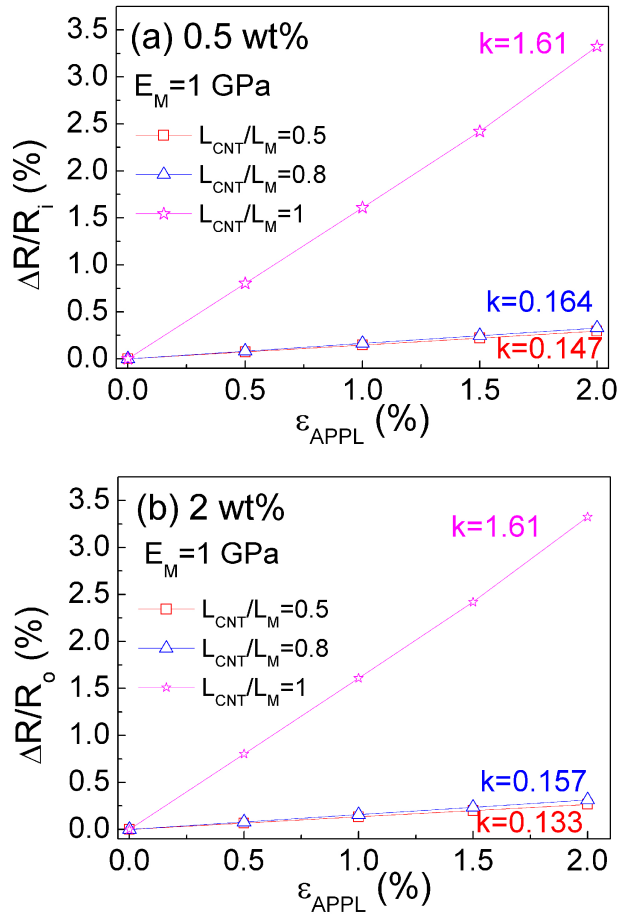

FIGURE 5. Normalized change in electrical resistance as a function of the applied strain. (a) 0.5 wt%, (b) 2 wt%.

much higher than that of the polymer matrix. L_{CNT}/L_M= 1 is, however, an unrealistic condition for most real CNT composites. It is also observed that α is very similar for 0.5 and 2 wt%, with a slight difference for the lower L_{CNT}/L_M ratios. The CNT deformation is weakly dependent on L_{CNT}/L_M for L_{CNT}/L_M= 0.1 to 0.9. The influence of the L_{CNT}/L_M ratio on the change of the composite electrical resistance under application of axial strain was then investigated. Using α calculated as in Fig. 4, $\Delta R/R_i$ was computed from Eq. (7) for different values of L_{CNT}/L_M and different ε_{APPL}, keeping E_M= 1 GPa, see Fig. 5.

The slope of the straight line is defined as the gage factor (k) and in this case quantifies the piezoresistive sensitivity of the composite due to the CNT deformation exclusively. This slope tends to increase (higher k) with increased L_{CNT}/L_M. By comparing Fig. 5(a) and Fig. 5(b), it is observed that k is slightly higher for composites with lower CNT concentration (0.5 wt%, Fig. 5(a)). A higher CNT concentration yields stiffer composites and, as a consequence, less CNT deformation. In both plots, the case L_{CNT}/L_M= 1 corresponds to the limit case for which the CNT length is of the same length as that of the matrix and hence ε_{APPL}= ε_{CNT} ($i.e.$ a continuous "fiber" composite), yielding the same value of k = 1.61 for both CNT concentrations. For a continuous conductive material that is axially stretched, an increase in L and a decrease in A (by Poisson's effect) will cause the electrical resistance to increase, provided that ρ is unaffected. The gage factor k yielded due to this purely geometric effect in a conductive wire is $k \approx 1 + 2\nu$, were ν is the Poisson's ratio [27,32]. For our case, ν of the CNT was taken as 0.3 and the geometric prediction is in remarkable agreement with our model in the limit case L_{CNT}/L_M= 1.

3.2. Influence of matrix elastic modulus

The influence of the matrix elastic modulus (E_M) on the CNT deformation and hence on the piezoresistive sensitivity of the composite was investigated. To obtain $\Delta R/R_i$, the CNT deformation (ε_{CNT}) and therefore α ($= \varepsilon_{CNT}/\varepsilon_{APPL}$) were first calculated for different values of E_M by the methodology described in Sec. 2.2 and then used in Eq. (7). Figure 6 shows $\Delta R/R_i$ vs. ε_{APPL} for three matrix moduli and L_{CNT}/L_M = 0.5. The CNT concentrations studied were 0.5 wt%, Fig. 6(a) and 2 wt%, Fig. 6(b), and the cases with E_M = 0.1, 1 and 10 GPa were investigated.

As observed from Fig. 6, k increases with increased matrix elastic modulus. The stiffness of the composite can be rationalized as a set of two springs connected in series, one representing the CNT and the second one the matrix. Hence, the total deformation is the sum of the deformation of the CNT and matrix. As the matrix stiffness increases (with ε_{APPL} remaining constant), the mismatch between the stiffness of the stiff CNT and compliant matrix is reduced, and more strain is shared by the CNT, yielding larger values of k.

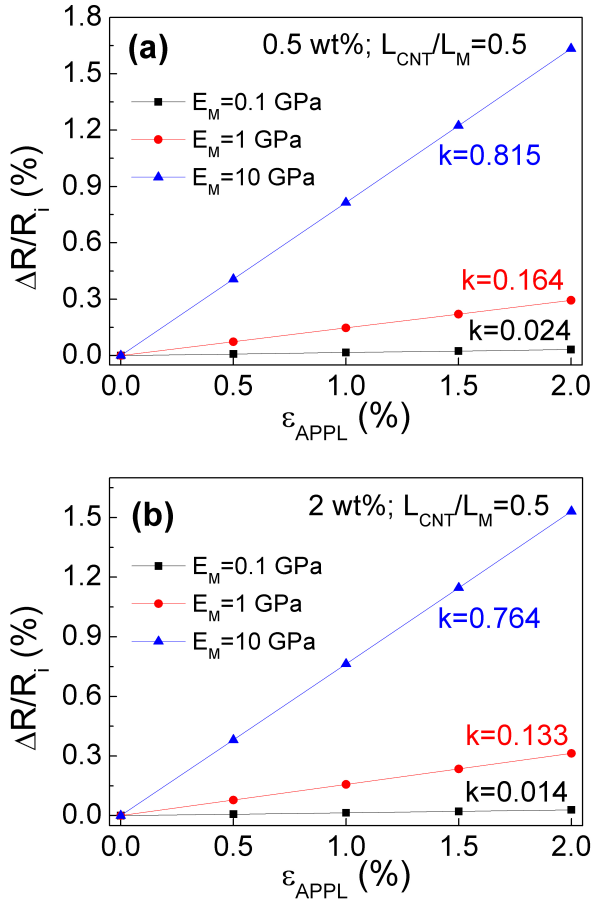

FIGURE 6.Normalized change in electrical resistance as a function of the applied strain for different matrix elastic moduli. (a) 0.5 wt%, (b) 2 wt%.

3.3. Influence of carbon nanotube orientation

Figure 7 shows $\Delta R/R_i$ vs $\varepsilon_{\text{APPL}}$ for CNTs oriented at different angles with respect to the applied strain and E_M= 1 GPa. In this figure, 0° represents the case where the CNT is aligned with the direction of the applied strain. It is observed that k is significantly larger when the CNT is aligned with the strain direction than when is not. When the CNT is oriented 30° with respect to the direction of $\varepsilon_{\text{APPL}}$, k is $\sim$ 60.5% of the maximum value corresponding to the aligned composite (k= 0.147), while for 60° k is only $\sim$ 6.8% of this maximum value. This behavior is explained by the larger CNT deformation which occurs when the CNT is aligned along the composite longitudinal axis.

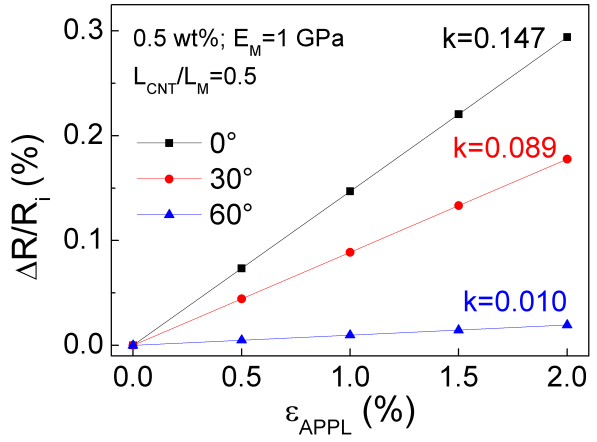

FIGURE 7. Normalized change in electrical resistance as a function of the applied strain for different CNT orientation with respect to the applied strain direction.

3.4. Comparison to experimental results

A previous experimentally studied CNT/polymer composite was modeled using the methodology proposed herein with the objective of quantifying the CNT deformation contribution to the total piezoresistivity of the actual composite. The experimental system consists of an axially strained 0.5 wt% MWCNT/polysulfone film [21]. The MWCNTs were aligned at the macroscale in the composite by application of an alternating electric field. Changes in the electrical resistance were monitored *in situ* while the film was strained, in order to measure the composite gage factor (k_{exp}). Further details of the experimental setup can be found in [21]. To model this system, FEA was conducted using the CNT properties listed earlier, a matrix elastic modulus and Poisson's ratio of E_M = 1.5 GPa and ν= 0.3 respectively, and CNT concentration as in the experimental system (0.5 wt%). The CNT was modeled aligned in the direction of the applied strain and L_{CNT}/L_M= 0.5, and the results are presented in Fig. 8. The slope of the linear fit of the experimental data in Fig. 8 represents the average measured gage factor of the tested composite (k_{exp}=2.68). On the other hand, Eq. (7) predicts a geometric gage factor (k_{geom}) of 0.15, which represents only $\sim$ 5% of the total piezoresistive sensitivity measured. Thus, the remaining $\sim$ 95% has to be related to changes in the network resistivity which has been explained in the literature in terms of CNT-to-CNT contact, variations in interparticle distances

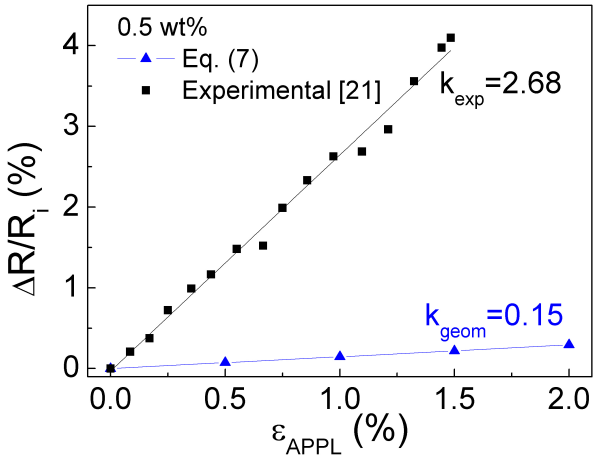

FIGURE 8. $\Delta R/R_i$ vs $\varepsilon_{\text{APPL}}$ for an aligned CNT/polysulfone composite. k_{exp} is the experimental composite gage factor measured in [21] while k_{geom} represents only the CNT deformation contribution predicted herein.

and tunneling resistances [22-26,33]. Therefore, the comparison between the proposed model and actual experiments suggests that the geometric effects caused by the actual deformation of the CNTs are minor compared to the effects related to changes in the CNT network configuration.

4. Conclusions

An analysis of the contribution of the CNT deformation to the piezoresistivity of CNT/polymer composites under unidirectional axial strain was developed. A simple analytical model which estimates the composite relative change of electrical resistance due to the applied strain at the macroscale was proposed. Finite element analysis was conducted to quantify the influence of the CNT deformation on the piezoresistive behavior of CNT/polymer composites. The influence of the CNT length, concentration, degree of alignment and matrix elastic modulus on the geometric piezoresistive sensitivity of the composite was investigated. The contribution of the CNT deformation to the piezoresistivity of polymer composites increases with increased CNT length, CNT alignment along the strain direction and matrix elastic modulus, while decreases with increased CNT concentration. For CNT/polymer composites with discontinuous CNTs ($L_{\text{CNT}}/L_M < 1$), this geometric contribution was estimated to be less than $\sim 5\%$ of the whole piezoresistive effect. Only for continuous CNTs ($L_{\text{CNT}}/L_M = 1$), the geometric contribution from the CNT deformation may significantly affect the piezoresistive response of the composite. Based on the presented results, it is concluded that the main responsible for the piezoresistive behavior of most CNT/polymer composites experimentally studied in the literature is the change in the configuration of the CNT network, rather than the changes in length and diameter of the CNTs themselves.

Acknowledgments

This work was supported by CONACYT (Mexico) through CIAM project No. 188089 Authors greatly appreciate the valuable comments of Dr. Gary D. Seidel from Virginia Tech.

1. T.W. Tombler *et al*., *Nature* **405** (2000) 769.
2. M.B. Nardelli and J. Bernholc, *Phys. Rev. B* **60** (1999) 16338.
3. P. Dharap, Z. Li, S. Nagarajaiah and E.V. Barrera, *Nanotechnology* **5** (2004) 379.
4. W. Zhang, J. Suhr and N. Koratkar, *J. Nanosci. Nanotechnol*. **6** (2006) 960.
5. I.P. Kang, M.J. Schulz, J.H. Kim, V. Sanov and D.L. Shi, *Smart. Mater. Struct.* **15** (2006) 737.
6. L.J. Lanticse *et al*., *Carbon* **44** (2006) 3078.
7. R. Haggenmueller, H.H. Gommans, A.G. Rinzler, J.E. Fischer, K.I. Winey, *Chem. Phys. Lett.* **330** (2000) 219.
8. J.R. Wood, Q. Zhao, H.D. Wagner, *Composites A* **32** (2001) 391.
9. E.T. Thostenson, T.W. Chou, *J. Phys. D: Appl. Phys.* **36** (2002) L77.
10. J.K.W. Sandler *et al*., *Polymer* **45** (2004) 2001.
11. P. Potschke, S.M. Dudkin, I. Alig, *Polymer* **44** (2003) 5023.
12. T. Kimura, H. Ago, M. Tobita, S. Ohshima, M. Kyotani, M. Yumura, *Adv. Mater.* **14** (2002) 1380.
13. B.W. Smith, Z. Benes, D.E. Luzzi, J.E. Fischer, *Appl. Phys. Lett.* **77** (2000) 663.
14. J. Hone J *et al*., *Appl. Phys. Lett.* **77** (2000) 666.
15. K. Yamamoto, S. Akita, Y. Nakayama, *J. Phys. D: Appl. Phys.* **31** (1998) L34.
16. M.S. Kumar, T.h. Kim, S.H. Lee, S.M. Song, J.W. Yang, K.S. Nahm, E.K. Suh, *Chem. Phys. Lett.* **383** (2004) 235.
17. J. Li, Q. Zhang, N. Peng, Q. Zhu, *Appl. Phys. Lett.* **86** (2005) 153116.
18. R. Krupke, F. Hennrich, H. Löhneysen, M. Kappes, *Science* **301** (2003) 344.
19. C. Park *et al*., *J. Polym. Sci. B* **44** (2006) 1751.
20. A.I. Oliva-Avilés, F. Avilés V. Sosa, A.I. Oliva, F. Gamboa, *Nanotechnology* **23** (2012) 465710.
21. A.I. Oliva-Avilés, F. Avilés and V. Sosa, *Carbon* **49** (2011) 2989.
22. N. Hu, Y. Karube, M. Arai, T. Watanabe, C. Yan, Y. Li, Y. Liu and H. Fukunaga, *Carbon* **48** (2010) 680.
23. T.C. Theodosiou and D.A. Saravanos, *Compos. Sci. Technol.* **70** (2010) 1312.
24. M.D. Rein, O. Breuer and H.D. Wagner, *Compos. Sci. Technol.* **71** (2011) 373.
25. C. Li, E.T. Thostenson and T.W. Chou, *Appl. Phys. Lett.* **91** (2007) 223114.
26. M.H.G. Wichmann, S.T. Buschhorn, J. Gehrmann and K. Schulte, *Phys. Rev. B* **80** (2009) 245437.
27. A.S. Kobayashi, *Handbook on Experimental Mechanics* (VCH Publishers, New York, 1993), p.40.
28. X.L. Chen and Y.J. Liu, *Comput. Mat. Sci.* **29** (2004) 1.
29. UDEL Polysulfone Design Guide, *Solvay Advanced Polymers* (2002).
30. P.G. Collins and P. Avouris, *Scient. Am.* **238** (2000) 62.
31. C. Li and T.W. Chou, *J. Nanosci. Nanotechnol*. **3** (2003) 423.
32. R.L. Hannah and S.E. Reed, *Strain Gage User's Handbook* (Elsevier Applied Science, London and New York, 1992). p. 4.
33. M. Park, H. Kim and J. Youngblood, *Nanotechnology* **19** (2008) 055705.